

NACA TN No. 1705

8155

NATIONAL ADVISORY COMMITTEE FOR AERONAUTICS

TECHNICAL NOTE

No. 1705

EXPERIMENTAL INVESTIGATION OF THE EFFECTS OF PLASTIC FLOW
IN A TENSION PANEL WITH A CIRCULAR HOLE

By George E. Griffith

Langley Aeronautical Laboratory
Langley Field, Va.



Washington

September 1948

0144966



TECH LIBRARY KAFB, NIM

AFMDC
TECHNICAL LIBRARY
AFL 2011



NATIONAL ADVISORY COMMITTEE FOR AERONAUTICS

TECHNICAL NOTE NO. 1705

EXPERIMENTAL INVESTIGATION OF THE EFFECTS OF PLASTIC FLOW
IN A TENSION PANEL WITH A CIRCULAR HOLE

By George E. Griffith

SUMMARY

Seven uniformly dimensioned 24S-T tension panels with a central circular hole were subjected to various loads in order to study the effects of plastic flow at the point of maximum stress concentration. The results, presented in graphical form, show that, as the amount of plastic flow increases, the stress concentration factor is appreciably reduced and the strain concentration factor is appreciably increased. Subjecting the panels to 100 repeated loading cycles caused no change to occur in the maximum values of the stress and strain concentration factors.

INTRODUCTION

In structural members, discontinuities such as holes produce stress concentrations but the effects of plastic flow on such stress concentrations, especially under repeated loads, are not generally known. Because the localizing of high stresses is believed to be the forerunner of failure under repeated loads (fatigue failure), stress concentrations are considered to be more serious in fatigue than in statics.

The purpose of the present investigation is to determine, for a simple case of stress concentration in a tension panel with a central hole, the effect of plastic flow in modifying the stress concentration factor and the range of stress during 100 loading cycles.

SYMBOLS

P	panel load, kips
ϵ	measured strain
σ_{av}	average net-section tensile stress due to external loading of panel that has not been previously subjected to a higher load, ksi

σ_C	compressive stress in direction of loading, ksi
σ_T	tensile stress in direction of loading, ksi
σ_{tr}	transverse tensile stress perpendicular to direction of loading, ksi

TEST SPECIMENS AND PROCEDURE

Test specimens.— The test specimens consisted of seven 24S-T aluminum-alloy panels approximately 0.091 inch thick, 24 inches wide, and 58 inches over-all in length, each with a central circular hole four inches in diameter. Actual panel dimensions are given in table 1.

Panel tests.— Nine tests were made, two of the panels being used for second tests. A complete test schedule is presented in table 2. For the seven initial tests the panels were subjected to 100 cycles of loading, each loading cycle consisting of loading from zero load to a specified maximum tensile load and unloading to zero load, at an average rate of approximately two cycles per minute. The maximum loads were varied so that the average net-section stress ranged from 23.5 ksi on panel 1 to 50.6 ksi on panel 7. Strains were measured at various load increments during loading and unloading for loading cycles 1, 3, 6, 10, 30, 60, and 100. All panels were tested in a 1200 kip testing machine (accurate to about 1/2 percent). Whipple-trees were used at each end of the panels to insure uniform loading. No restraint against buckling was provided except in test 7 wherein roller bearings were used at six points on the panel.

For the eighth test, panel 2 (original maximum load = 45.9 kips, $\sigma_{av} = 25.5$ ksi) was retested through four additional cycles in which the maximum loads were successively 45.5 kips, 55.0 kips, 65.0 kips, and 75.0 kips. For test 9, panel 4 (initial maximum load = 63.7 kips, $\sigma_{av} = 36.0$ ksi) was retested by loading once to 63.7 kips, once to 91.0 kips ($\sigma_{av} = 51.3$ ksi), and then through 100 additional cycles with the maximum load again at 63.7 kips.

Strain measurements.— Three types of gages were used for measuring strains. Electromagnetic strain gages designed specifically for accurate results at high strains (having an accuracy of about 1.5 percent throughout the strain range encountered in the test) were used to measure the maximum strain concentrations. These gages, of both $\frac{1}{2}$ -inch and 1-inch gage lengths, were placed inside the hole across the transverse axis but the 1-inch gages were used only in tests 1 and 2, the $\frac{1}{2}$ -inch gages being used in the remaining tests. According to the

theoretical elastic strain distribution (reference 1) at the edge of the hole, the $\frac{1}{2}$ -inch gage length would produce an error of 2.5 percent below the maximum strain, and the 1-inch gage would be in error by 7.5 percent. All results given in the text for maximum stress and strain concentrations are taken from the $\frac{1}{2}$ -inch gages, but no corrections have been made to the original strain readings. The extent to which plastic flow modifies the error of 2.5 percent for strains is not known, but in the conversion of strains to stresses the error would tend to be minimized. No correction is necessary for having read the strains across the $\frac{1}{2}$ -inch chord rather than the arc.

One-half inch Baldwin Southwark SR-4 type A-5 electric wire gages were attached to all panels except panel 7 at stations along the transverse axis (across the net section) to check the net-section strain (or stress) distribution. These gages are probably accurate within about 2 percent up to a strain of 0.0024 but are somewhat less accurate at higher strains. (See references 2 and 3.) Since the wire gages are calibrated to include a normal Poisson effect, the accuracy of these gages is also affected if the transverse strains are appreciably different from the value indicated by Poisson's ratio.

Stress-strain tests.— Before the panel tests were begun, standard tension coupons were cut from excess material at the four corners of each test panel and stress-strain tests were made to establish the material properties of the panels.

After the panel tests were completed, auxiliary stress-strain tests were needed to convert the strain histories of all fibers inelastically strained and of those fibers inelastically strained in both tension and compression into stress histories. Coupons were again obtained from material at the four corners of the panels. A test procedure employing lubricated steel guides similar to the procedure of Bruggeman and Mayer

(reference 4) was used, with strains being measured by the $\frac{1}{2}$ -inch electromagnetic gages. In order to reproduce the strains of the panel tests the coupons were subjected to continuous cycles of strain. Starting at zero strain, the specimens were stretched to a desired maximum tensile strain, the strain was reduced and the specimens were compressed to a desired maximum compressive strain, then strained again to the maximum tensile strain, and so on. When the strain in a coupon equalled the measured strain obtained from the individual histories of the panel tests, the load thus determined was recorded. From these loads the coincident stresses were obtained. In this manner strain histories of the individual panels, for the first few cycles of loading, were translated into stress histories.

TEST RESULTS

The stress-strain relation is a very simple one as long as Hooke's law applies but becomes quite complicated when plastic flow develops; in the plastic range, stress characteristics in general are then quite different from strain characteristics. The discussion is therefore divided into two parts, one for elastic behavior, the other for inelastic behavior. In the first part, which is concerned with elastic action, no distinction is necessary between stresses and strains; hence it will be unnecessary to mention strain. In that part of the discussion dealing with plastic action it is perhaps more logical to discuss the strain results first, for the strains were actually measured, whereas the stresses must be converted from these strains.

Elastic Behavior

Stress concentration factor.— The theoretical maximum value of the stress concentration at the edge of a circular hole in a straight tension member of infinite width is three times the applied uniform stress (reference 1). Coker and Filon (reference 1) regard this value as approximately correct whenever the plate width is four or more times the hole diameter, and Timoshenko (reference 5) concurs with this opinion if the width is five or more times the diameter. Since the ratio of plate width to hole diameter was six for the test panels, a theoretical stress concentration factor of 3.00 can be accepted. The value obtained experimentally (average of 5 tests during the first cycle of loading in the elastic range) was 3.08 (2.7 percent higher than the theoretical value).

In terms of net-section stress, which provides perhaps a more desirable comparison in dealing with static stress analysis, when the plate width is six times the hole diameter, the theoretical stress concentration factor becomes 2.50. The corresponding experimental value (5 tests) was 2.57. Available photoelastic results (reference 1) also give stress concentration factors slightly higher than the theoretical values, but these results are for smaller width-diameter ratios.

Stress distribution across the net section.— When all fibers are strained elastically only, the theoretical and experimental stress distributions are in good agreement. Such a comparison is shown in figure 1 which contains representative test results. The area under a smooth curve drawn through the test points — that is, the total integrated stress over the cross section — is 2.9 percent below the applied load. For six tests in the elastic range the integrated experimental stress varied from 0.5 to 4.5 percent less than the applied load, the average being 2.4 percent low.

As can be seen from figure 1, all the test points derived from the wire-gage readings fall slightly below the theoretical curve, a consistent tendency throughout the tests. This result may be due in part to inherent inaccuracy of the gages (reference 2) and a tendency for these gages to read low when not prestrained. Serving to offset any tendency for low strain readings is the presence of transverse tensile strains (or stresses) instead of the compressive strains (Poisson effect) for which the wire gages in tension are calibrated. These transverse stresses cause the gages to give stresses higher than the true tensile stresses. The gages are most affected where the transverse stress is appreciable in comparison with the tensile stress in the direction of loading. The theoretical distributions (reference 1) for both types of stress are shown in figure 2, and the region of greatest error is found to extend from approximately $\frac{1}{2}$ inch to 3 inches from the edge of the hole. This error due to transverse stresses has a maximum value of about 2 percent.

Indicative of the over-all accuracy of the measurements, regardless of the loading conditions or whether the strains were elastic or inelastic, is the result that, throughout the tests, at loads greater than 30 kips the integrated experimental stress over the net section always agreed within 5.0 percent of the applied load. At the lowest loads (including zero load) the integrated stress always agreed within 3.0 kips of the applied load.

Range of stress.— In fatigue studies the range of stress (or strain) is customarily defined as the change in stress (or strain) as the load changes from a maximum to a minimum through succeeding cycles. The change from an initial state of no stress to the maximum stress is neglected. In the present paper, the range of stress (or strain) is discussed only for the most highly stressed fibers, that is, for the point of maximum concentration.

As long as the action is elastic, the range of stress is 2.57 times the average net-section stress range or 3.08 times the average gross-section stress range.

Plastic Behavior

Strain and stress concentration factors.— In figure 3 are shown strains measured by the $\frac{1}{2}$ -inch electromagnetic gages for four tests during the first loading cycle. Other test results and strains measured during succeeding cycles have been omitted for clarity of the figure. The smooth curve drawn through the test points from the origin to point E represents the average of all the strains obtained as the initial panel loads were increased. The strain and stress concentration factors are based upon this curve.

In order to convert these experimental strains to stresses, use was made of both the original and the auxiliary stress-strain tests. The test curve from the origin to point E in figure 4 was obtained as part of the auxiliary tests, but it also represents the average tension curve of both the original and auxiliary tests. The maximum scatter at the tension knee of the auxiliary tests is shown, but some test results and all test points have been omitted for clarity. Thus the strains shown by the average curve from the origin to point E in figure 3 correspond to the stresses shown by the curve from the origin to point E in figure 4. These average curves were used in calculating the stress and strain concentration factors given in figure 5.

Although figure 3 shows test values obtained only in the first cycle, the same maximum strains (within the scatter of experimental error) were obtained in the 99 succeeding cycles when the same maximum loads were applied to the individual panels. The strain concentration factor simply repeated itself through succeeding cycles when the same maximum panel load was applied. In the auxiliary tests, the coupons were loaded cyclically only a few times, but repeating the same maximum strains brought about a repetition of the same maximum stresses. From this result the stress concentration factors are concluded to be the same for succeeding cycles.

After the load of 91.0 kips had been applied to panel 4 in test 9, the strain increments in succeeding cycles due to the load of 63.7 kips were purely elastic, as from point F to point F' (and back to point F) in figure 3. Therefore, values of strain or stress concentration factors are given only for original panel loading conditions or for the condition when the original maximum load was exceeded.

As can be seen from figure 5, plastic flow decreases the stress concentration factor but markedly increases the strain concentration factor. The stress concentration factor decreases from an elastic value of 2.57 to about 1.21 as the average net-section stress is increased to 50 ksi, whereas the strain concentration factor increases from 2.57 to about 7.10.

Strain and stress distribution across the net section.— Figure 6 shows the change in strain distribution as the initial loads on the panels were increased. This figure was constructed by plotting the strains obtained in the tests during loading of the first load cycle (as, for example, the stresses were plotted in figure 1). Each succeeding test gave a check on most previous test points; that is, the maximum load in test 6 was greater than in test 5 and consequently the strains of test 6 traced the strains of test 5 and extended to higher strains. The top surface of the figure was then obtained by drawing smooth curves through these test points. The test results were very consistent, very little scatter occurring in the test points.

Figure 7 was obtained by connecting the strains (or test points) measured when the load, during the first loading cycle, returned to zero. Figure 7, therefore, represents the net amount of stretching or elongation remaining when the panel load has been released. The over-all change in strain, as the load varied from a maximum to zero, would be obtained by subtracting the strains of figure 7 from those of figure 6. The strains of figure 7 cannot be converted to stresses without tracing the original complete strain histories on comparable stress-strain curves. For example, in figure 3 the strain at F represents a net positive elongation, yet in figure 4 the same strain is equivalent to a compressive stress. In figure 7 the strains (or the curve) at zero distance from the edge of the hole are the values obtained at the intersection of the zero load axis and the straight lines AB, CD, and EF of figure 3. Test 7 is not included in figure 7, no gages having been attached along the net section of panel 7. These zero load strains will be discussed more fully in the next section.

The results shown in both figures 6 and 7 are probably somewhat more affected by transverse tensile strains in the region away from the edge of the hole than are the results in the elastic range. Reference 6 shows that Poisson's ratio tends to increase slightly with increase of plastic strain. In contrast to the 2.0 percent maximum error in strain readings in the elastic range, the probable maximum error for the plastic strains amounts to about 3.0 percent. The resistance-type wire gages are also somewhat less reliable at higher strains (reference 3).

Figures 8 and 9 show the stress distributions corresponding to the strain distributions given in figures 6 and 7. The strains used in obtaining figure 6 were translated into stresses with the aid of the curve from the origin to point E in figure 4. These data were plotted and the points connected to give the surface shown in figure 8. In order to obtain figure 9 it was necessary to trace the strain history of each test point in the manner of the history represented by the circles in figure 3 from the origin to point A to point B, and then with the aid of the auxiliary tests of figure 4 to follow this strain and read the stress at the end of the loading cycle. Even if all the auxiliary test results were shown, some interpolation would be necessary in obtaining figure 9.

During succeeding cycles the strain readings varied from the minimum values shown in figure 7 to the maximum values shown in figure 6, and the corresponding stresses varied from the minimum shown in figure 9 to the maximum shown in figure 8. For both tests 8 and 9 the strain and stress distributions produced under the new maximum loading cycles were in good agreement with the corresponding distributions given in figures 6 to 9.

In addition to showing the effects of plastic flow on the strain and stress distributions across the net section, figures 6 and 8 also give some idea of the effect of plastic flow on the strain and stress gradients.

Range of strain and stress at the point of maximum stress concentration.— Before the experimental results are analyzed it is desirable to discuss some of the factors involved.

When a fiber in a region where stress concentration is not present is first strained plastically, work is done in stretching the fiber, and the yield point in the direction of stretching is increased. If the load causing the strain is released, the loss in strain will approximately follow Hooke's law, and if a load of opposite sign is applied it will generally be found that the yield point in the second direction has been decreased (Bauschinger effect — see, for example, reference 5). This effect is found in most ductile materials, but the compressive yield strength for some materials begins to increase again after the material has been subjected to appreciable permanent set. Reference 7 shows that for 24S-T this set is about 2.2 percent. For 24S-T material, the net result as the amount of permanent set increases is a gradual increase in the sum of the absolute values of the tension and compression yield strengths and a very gradual increase in the sum of the tension and compression proportional limits (reference 7). Whether this effect is present in the test panels at the point of maximum stress concentration and, if so, to what extent, is unknown. The influence of the straining at different rates of adjacent fibers is not known. These effects cannot be evaluated from the test data.

Figure 3 shows that, as the load on the panels returned to zero, the strain readings for some tests deviated from a straight-line return (as, for example, the test points from C to D in test 6). Since the panels were not restrained from buckling, except partially in test 7, this deviation shows no consistent trend. Fibers strained inelastically in tension will usually lose strain more rapidly beyond the point where the elastic limit (determined by the Bauschinger effect) is reached (as, for example, from D' to D in figure 4). In the panel tests the influence of surrounding fibers, the absence of restraint against buckling, and other factors of unknown quantity make it impossible to determine accurately the return strains at zero load. Because of this uncertainty, the return strains at zero load which were used in the calculations and in figure 7 are the strains obtained from the intersections of the straight lines drawn through the test points (CD in figure 3) and the zero load axis. In test 7 the error thus involved might be appreciable; in the other tests it is probably quite small.

Two sources of error are present in figure 3. The first is a slight difference between the maximum measured strain for any particular test and the strain corresponding to the same maximum load on the straight line through the test points as the panel unloaded. The same effect to the same degree was experienced in the auxiliary tests but is not shown in figure 4. This effect is believed to be due to the electromagnetic gages, for it occurred consistently when these gages were used whenever the direction of load changed but did not occur when the wire gages were used. The second source of error concerns the slopes of

the lines from A to B, from C to D, and from E to F. These slopes tend to become gradually shallower as the maximum strain is increased. This result was evident for both the panel tests and the auxiliary tests, and the percentage change in slope for the panel tests was in excellent agreement with the percentage change in slope for the auxiliary tests. This change in slope is mainly a result of the error in strain readings caused by the change in gage length; large strains change the original gage length and the true unit strain is thereby affected.

The ranges of stress and strain depend upon the factors discussed in the foregoing paragraphs. These ranges are shown in figure 10. The actual stress and strain range curves were based on the experimental results which led to figures 3 and 4 in the manner already described. For purposes of comparison fictitious elastic stress and strain range curves are also shown. These curves show the ranges that would occur if Hooke's law prevailed. The actual strain range is seen to increase slightly more than the (fictitious) elastic strain range at the point where plastic flow develops. The actual stress range begins to fall below the (fictitious) elastic range of stress at the point where the Bauschinger effect comes into force.

Also included in figure 10 for comparison are stress and strain range curves based on the stress or strain concentration factor. Should the statement that plastic flow reduces stress concentration and increases strain concentration and the curves of figure 5 be taken too literally and applied to range of stress or strain without first studying figures 3 and 4, the result would be the two extreme or outermost curves shown in figure 10. Since these curves are based only on the stress or strain concentration factor, they merely represent the change in stress or strain during the first half of the initial load cycle and consequently not the actual stress or strain ranges. In order to find the actual ranges, the complete strain history and the basic behavior (the true stress-strain relationship) of the fibers undergoing concentration must be known throughout the loading cycle.

Figure 10 gives results for the first cycle only, but the test results showed that the actual strain ranges for succeeding cycles remained essentially constant. The actual stress ranges are likewise assumed to remain constant. The results of tests 8 and 9 which were for strain and stress ranges different from the initial test ranges, were in good agreement (within 4.0 percent) with the corresponding values of figure 10 when the correct maximum loads were applied to the panels.

CONCLUSIONS

A study of the experimental data indicated that, for the 24S-T aluminum-alloy panels tested:

1. Within the elastic range, the theoretical and experimental results were in good agreement.

2. As the amount of plastic flow increased, the stress concentration factor (based on the average net-section stress) decreased from 2.57 to 1.21 when the average net-section stress reached a value of 50 ksi, while the strain concentration factor increased from 2.57 to 7.10.

3. Within the experimental scatter, the test results were not changed in 100 cycles by repeating the loading cycles.

Langley Aeronautical Laboratory
National Advisory Committee for Aeronautics
Langley Field, Va., May 25, 1948

REFERENCES

1. Coker, E. G. and Filon, L. N. G.: A Treatise on Photo-Elasticity. Cambridge Univ. Press (London), 1931.
2. Campbell, William R.: Performance Tests of Wire Strain Gages. I -- Calibration Factors in Tension. NACA TN No. 954, 1944.
3. Campbell, William R.: Performance Tests of Wire Strain Gages. III -- Calibrations at High Tensile Strains. NACA TN No. 997, 1945.
4. Brueggeman, W. C., and Mayer, M., Jr.: Guides for Preventing Buckling in Axial Fatigue Tests of Thin Sheet-Metal Specimens. NACA TN No. 931, 1944.
5. Timoshenko, S.: Strength of Materials, Part II -- Advanced Theory and Problems. Second ed., D. Van Nostrand Co., Inc., 1941.
6. Stang, Ambrose H., Greenspan, Martin, and Newman, Sanford B.: Poisson's Ratio of Some Structural Alloys for Large Strains. Res. Paper RP1742, Nat. Bur. of Standards, Jour. Res., vol. 37, Oct. 1946, pp. 211-221.
7. Templin, R. L., and Sturm, R. G.: Some Stress-Strain Studies of Metals. Jour. Aero. Sci., vol. 7, no. 5, March 1940, pp. 189-198.

TABLE 1.— PANEL DIMENSIONS

Panel	Sheet thickness (in.)	Width (in.)	Hole diameter (in.)	Gross-section area (sq in.)	Net-section area (sq in.)
1	0.0895	23.95	3.998	2.144	1.786
2	.0898	24.04	3.998	2.159	1.800
3	.0891	24.05	4.000	2.143	1.786
4	.0886	24.00	3.999	2.126	1.772
5	.0892	23.99	3.998	2.140	1.784
6	.0892	24.00	3.998	2.141	1.784
7	.0882	24.00	3.999	2.117	1.764



TABLE 2.— TEST SCHEDULE

Test	Panel	Maximum load (kips)	Average net-section stress (ksi)	Number of cycles maximum load applied
1	1	41.9	23.5	100
2	2	45.9	25.5	100
3	3	54.9	30.7	100
4	4	63.7	36.0	100
5	5	72.8	40.8	100
6	6	81.9	45.9	100
7	7	91.0	50.6	100
8	2	45.5	25.3	1
		55.0	30.6	1
		65.0	36.1	1
		75.0	41.7	1
9	4	63.7	36.0	1
		91.0	51.3	1
		63.7	36.0	100



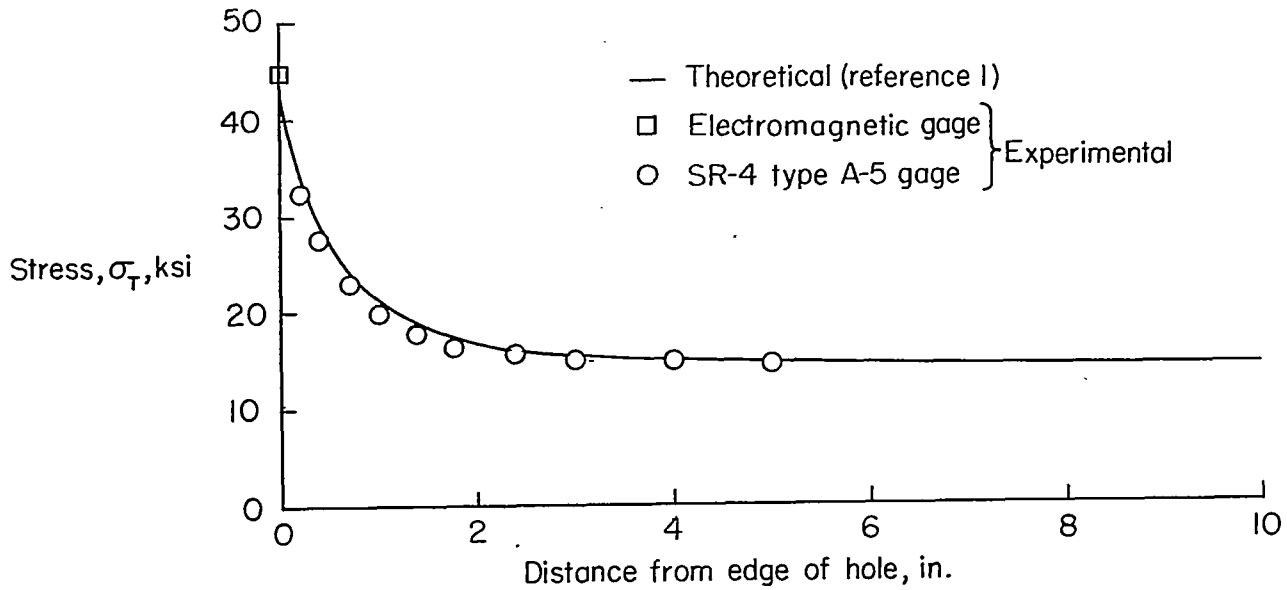


Figure 1.—Net-section tensile stress distribution typical of results obtained in elastic range. $P=30$ kips; $\sigma_{av}=16.4$ ksi.

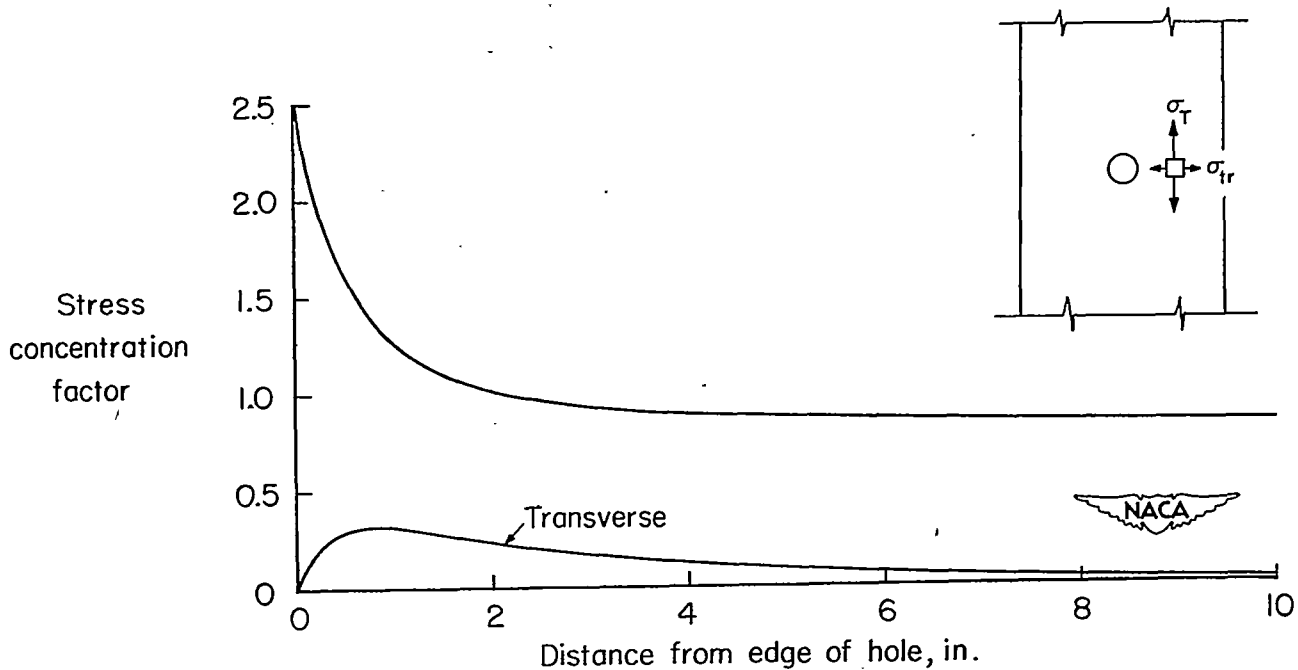


Figure 2.—Theoretical stress concentration factors (based on average net-section stress) for tensile stress and transverse tensile stress across the net section. (Reference 1.)

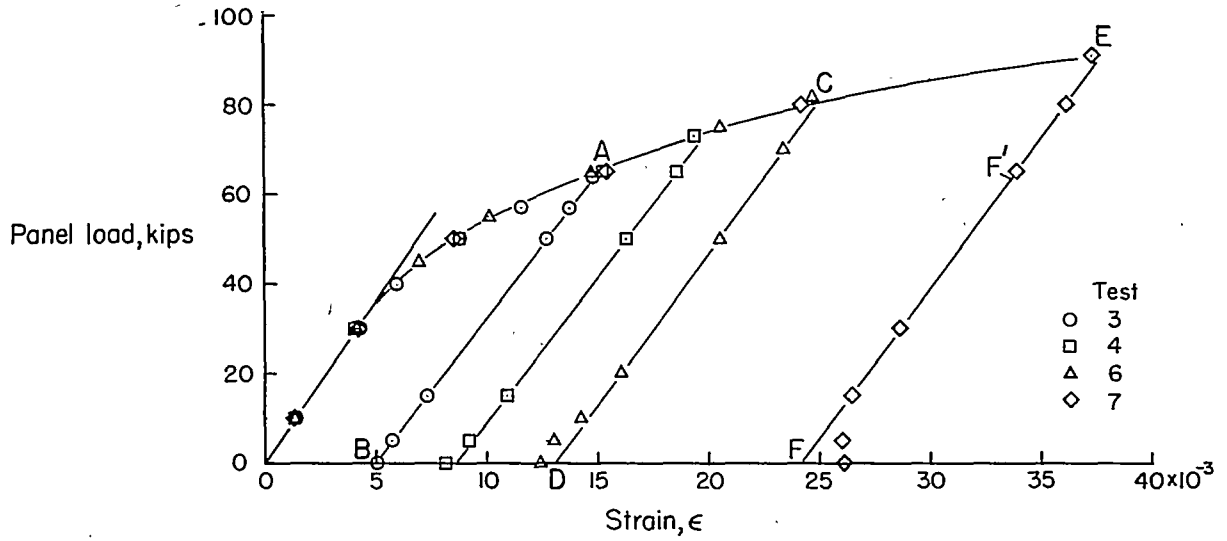


Figure 3.- Strains measured by the $\frac{1}{2}$ -inch electromagnetic gages during the first load cycle at point of maximum strain concentration.

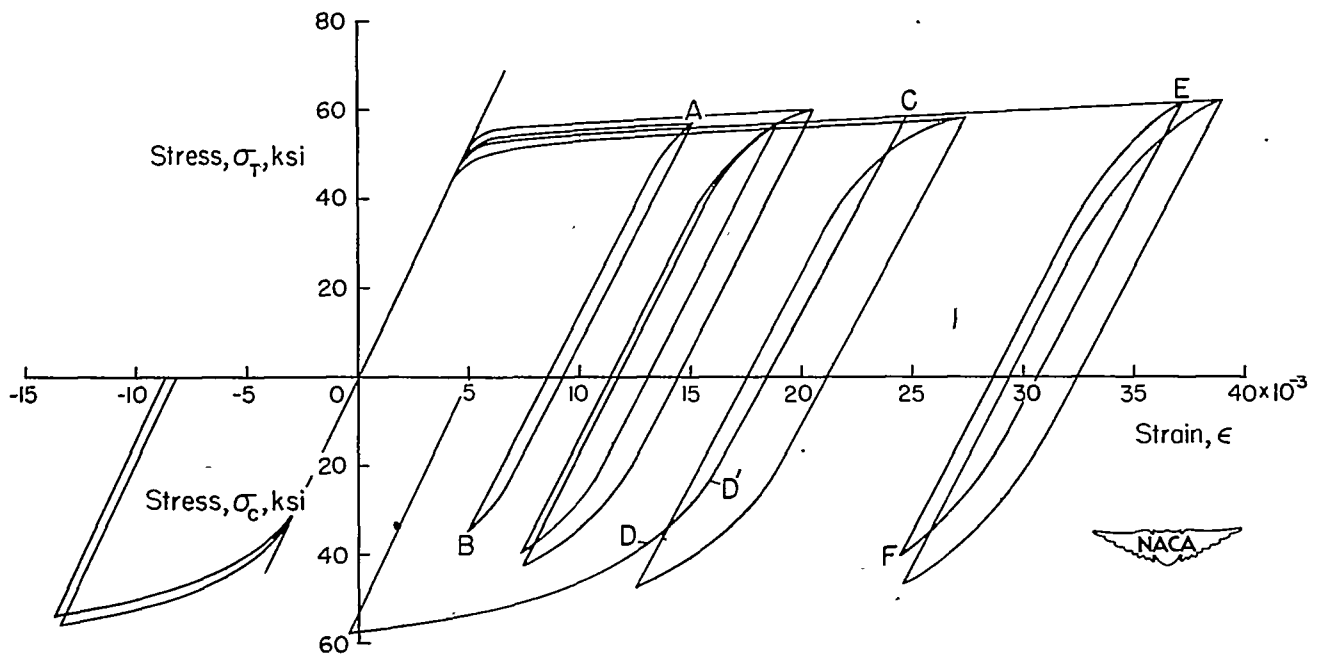


Figure 4.- Auxiliary-test results showing stress histories for fibers inelastically strained.

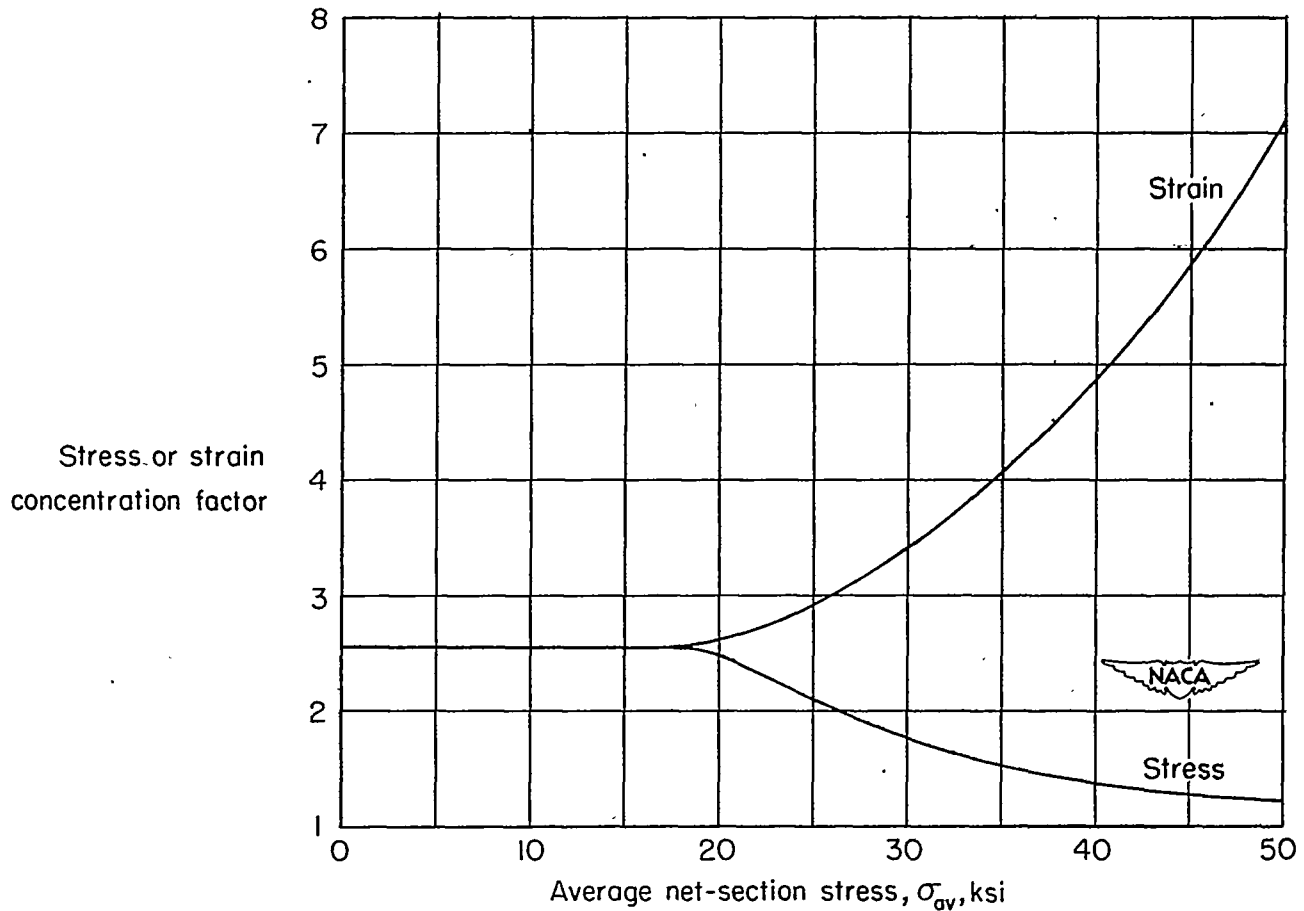


Figure 5.— Stress and strain concentration factors for first load cycle.

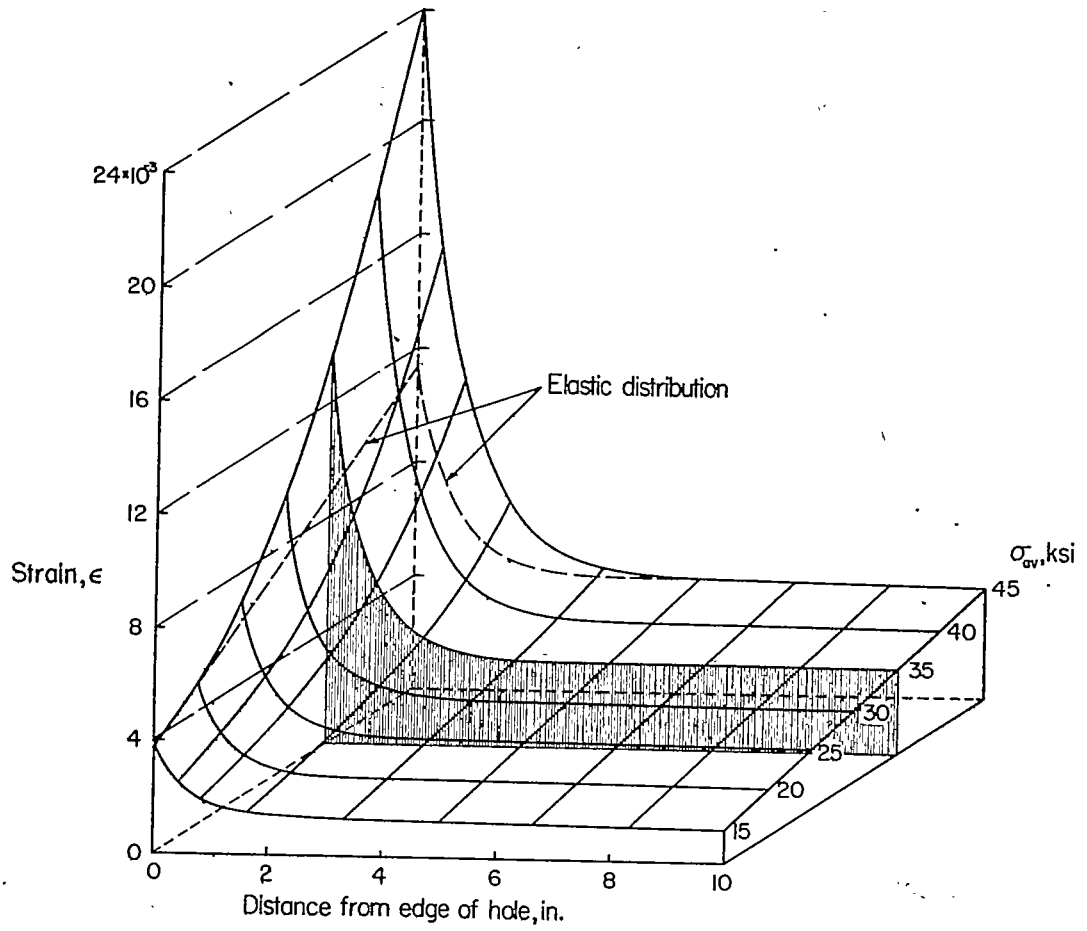


Figure 6.—Variation of net-section strain distribution with increase in load (first cycle).

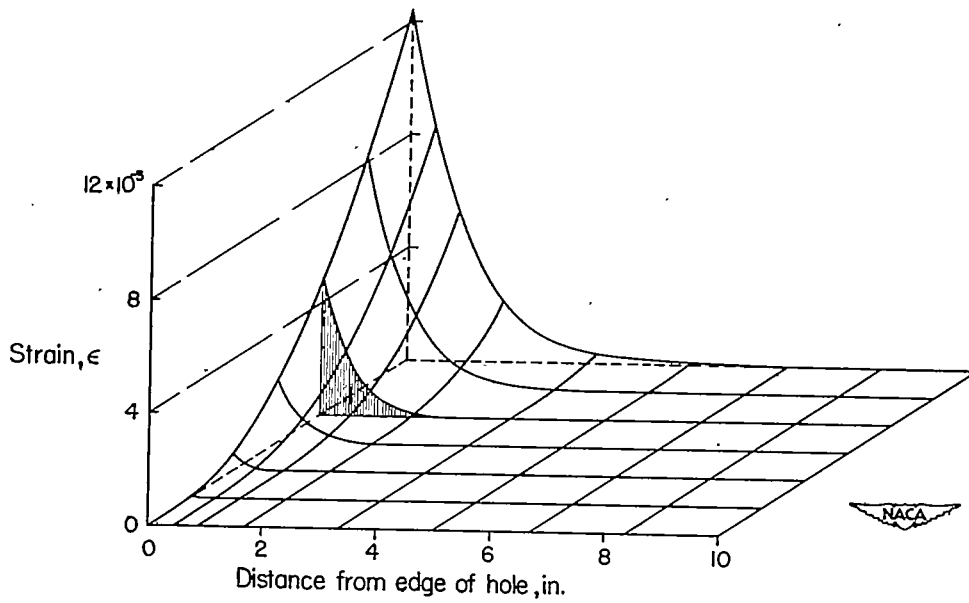


Figure 7.—Variation of net-section stress distribution at return to zero load (first cycle).

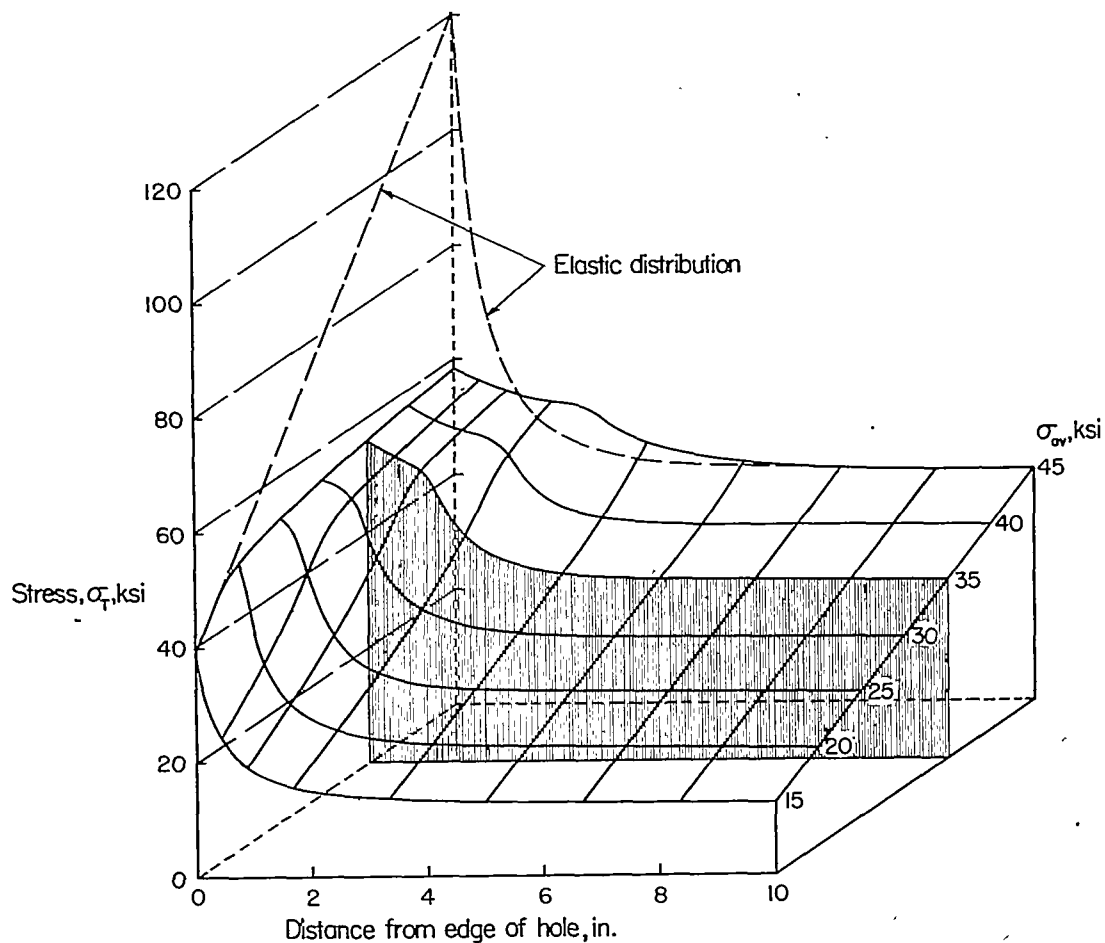


Figure 8.- Variation of net-section stress distribution with increase in load (first cycle).

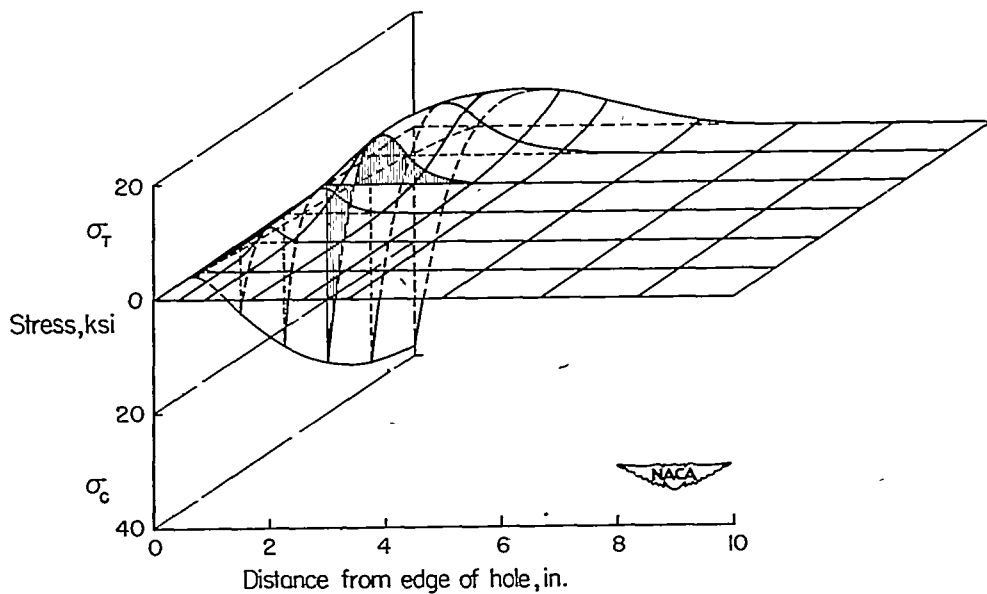


Figure 9.- Variation of net-section stress distribution at return to zero load (first cycle).

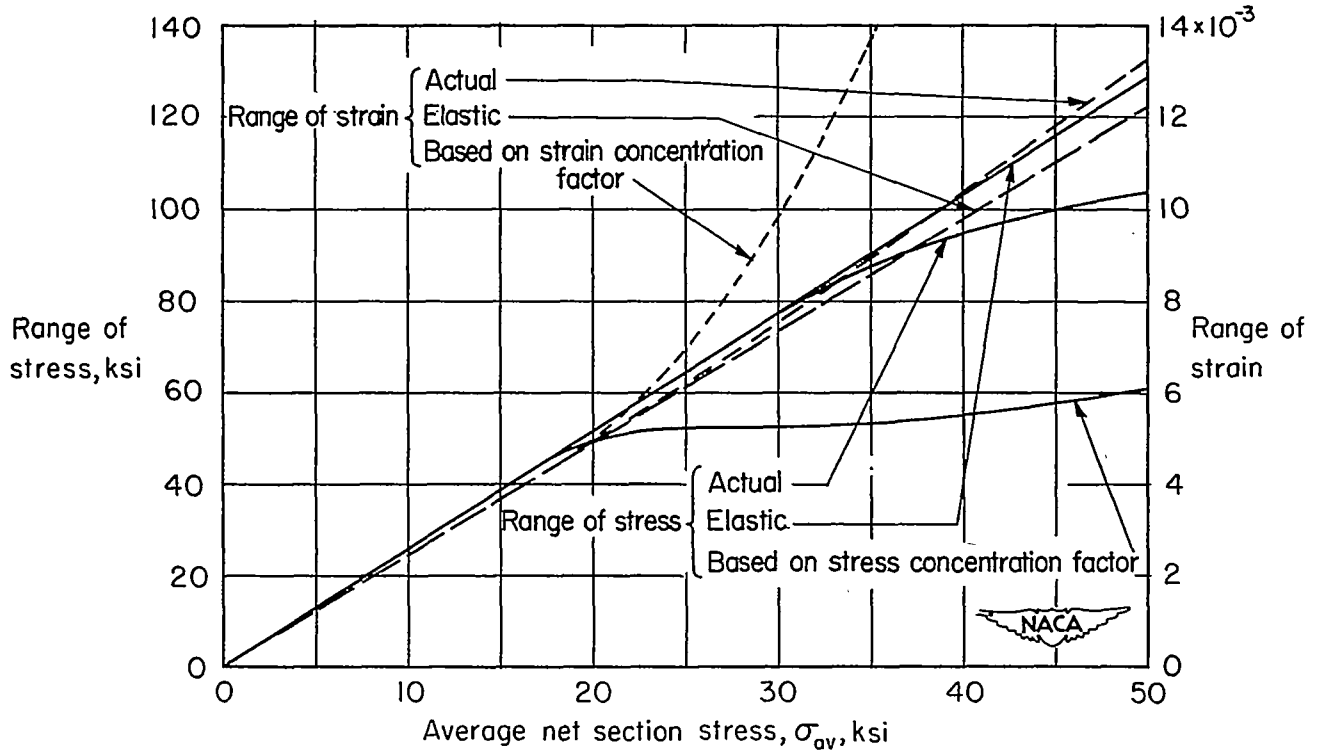


Figure 10.—Ranges of stress and strain at point of maximum concentration.